Matrix isolation studies of 185 nm light-induced cage reactions of *o*-chlorobenzaldehyde

Nobuaki Tanaka*, Hiroki Fujiwara, Haruki Ogawa, Hiromasa Nishikiori

Department of Environmental Science and Technology, Faculty of Engineering, Shinshu University, 4-17-1 Wakasato, Nagano 380-8553, Japan

* Corresponding author. Fax: +81-26-269-5550

E-mail address: ntanaka@shinshu-u.ac.jp (N. Tanaka)

Abstract

VUV light photolysis of *o*-chlorobenzaldehyde (CBA) has been investigated by infrared spectroscopy in cryogenic Ar and O_2 matrices. Previously reported photoinduced rotational isomerization from *anti*- to *syn*-CBA was confirmed in the Ar matrix. In addition, absorption bands associated with photoinduced rearrangement to benzoyl chloride were observed accompanying the weak bands due to the CO photolysis product. However, in the reactive O_2 matrix, isomerization was observed and there was no evidence of benzoyl chloride formation. A kinetic analysis revealed that rearrangement was a minor process under the present excitation energy. The TD-B3LYP calculations show that as the excitation energy increases the predissociation channel will open and the repulsive $^1(\pi, \sigma^*_{C–Cl})$ and $^1(n, \sigma^*_{C–Cl})$ states are directly achievable by the 185 nm excitation. Photoinduced rearrangement will be caused by the reaction of thus dissociated cage pairs.

Keywords: *o*-Chlorobenzaldehyde; Benzoyl chloride; Photolysis; Cryogenic matrix

1. Introduction

Photodissociation of C–Cl bonds in chlorinated benzene derivatives has been extensively studied [1-4], and these studies have indicated a complicated dissociation mechanism involving multiple channels and different excited states. The photodissociation mechanism of chlorotoluene upon 193 nm excitation has been proposed to involve three pathways: (1) direct dissociation or rapid predissociation, (2) predissociation through the triplet state and (3) predissociation via highly excited vibrational levels of the ground electronic state [2].

In a matrix, the photodissociation process is affected by the matrix cage wall [5, 6]. Sufficient excess translational energy of the atoms during photolysis is required for them to exit the cage. For heavy atoms such as Cl and Br, the diffusion process becomes more difficult [7]. In these cases, recombination, isomerization and reaction between dissociated cage pairs become important processes [8, 9].

Akai *et al*. reported the photoinduced rotational isomerization of *o*-chlorobenzaldehyde (CBA) in an Ar matrix [10]. Upon irradiation ($\lambda > 300$ nm) the isomerization from *anti*- to *syn*-CBA was the dominant process. They concluded that the rotational isomerization occurred at vibrationally excited states of T_1 after intersystem crossing from S_1 to T_1. However, the photochemistry of CBA in higher excited states has not yet been cleared in low temperature matrices.

In the present study, we report on the photochemical reactions of *o*-chlorobenzaldehyde in cryogenic matrices upon VUV irradiation. We also performed TD-B3LYP calculations to elucidate the excited state character. Furthermore, reaction rate constants are derived by measuring the absorbance changes of *anti*- and *syn*-CBA and a photoproduct to clarify the reaction mechanism.

2. Experimental

Light irradiation was performed using a low-pressure mercury arc lamp (HAMAMATSU L937-02, $\lambda > 185.0$ nm or L937-04, $\lambda > 253.7$ nm). IR spectra were measured in the range 4000–700 cm^{-1} with 1.0 cm^{-1} resolution by using a SHIMADZU 8300A Fourier transform IR spectrometer with a liquid nitrogen-cooled MCT detector. Each spectrum was obtained by scanning over 128 times. A closed-cycle helium cryostat (Iwatani M310/CW303) was used to control the temperature of the matrix.

Argon (Nippon Sanso, 99.999%) and O_2 (Okaya Sanso) were used without further purification. *o*-Chlorobenzaldehyde (Kanto Chemical, guaranteed reagent grade) was used after freeze-pump-thaw cycling at 77 K. Benzoyl chloride and chlorobenzene (Wako Pure Chemicals, S grade) were used as authentic samples for product identification. Samples were deposited on a CsI window at 6 K.

For product identification and energetic considerations, DFT calculations were utilized. Geometry optimizations were performed using Becke's three-parameter hybrid density functional [11] in combination with the Lee–Yang–Parr correlation functional, B3LYP [12] with the 6-311++G(2d,2p) basis set. Harmonic vibrational frequency calculations were performed to confirm the predicted structures as local minima or transition states and to elucidate the IR intensities. Potential energy curves along the C–Cl bond dissociation coordinate of *anti*-CBA were obtained by stepwise optimization with the fixed C–Cl bond length of the ground state and subsequent vertical excitation energy calculation at the TD-B3LYP/6-311++G(2d,2p) level. All calculations were performed using Gaussian 09 [13].

3. Results and discussion

3.1. Photolysis of CBA in the Ar and O_2 matrices

A mixture of CBA/Ar was deposited on a CsI window (CBA/Ar = 1/1000). In the infrared spectrum obtained after deposition, strong bands were observed at 1710 and 1705 cm^{-1}, which can be assigned to C=O stretching vibration of *anti*-CBA [10]. Fig. 1 shows the infrared difference spectrum obtained by the Hg-lamp irradiation (λ > 185.0 nm) irradiation of a CBA/Ar matrix for 120 min. The positive and negative bands indicate growth and depletion, respectively, during the irradiation period. Table 1 lists the observed wavenumbers of the growth bands. The positive bands at 1730, 1404, 1298, 1074, 846 and 755 cm^{-1} and the negative bands at 1710, 1705, 1269, 1058, 1056, 826 and 760 cm^{-1} are in good agreement with those of *syn*- and *anti*-CBA, respectively [10]. In addition to the peak growth bands due to the isomerization from *anti* to *syn* conformers, a band at 880 cm^{-1} showed continuous growth accompanied with bands at 1785, 1781, 1744, 1455, 1317, 1211, 1176, 778 and 776 cm^{-1}. The relative intensities of the bands remained constant during the irradiation period. These absorption bands could potentially be attributed to a single photoproduct (species A). The band at 1785 cm^{-1}, which could be assigned to the typical C=O stretch vibration showed a higher C=O wavenumber as compared with those of *anti*- and *syn*-CBA, indicating a strengthening of the C=O force constant, probably due to an electron attracting group attached to the carbon atom. In general, an acid chloride or anhydride is a plausible candidate. However, the anhydride can be ruled out owing to the present matrix ratio. To identify species A, an infrared spectrum of an authentic sample of Ar-matrix-isolated benzoyl chloride was measured, also shown in Fig. 1 in scaled absorbance. The strongest band (880 cm^{-1}) is assigned to the C–Cl stretch vibration [14]. The wavenumbers of species A are consistent with those of benzoyl chloride. Hence species A is identified with benzoyl

chloride. The weak band at 2139 cm^{-1} is due to CO [15]. Weak bands at 2120, 741 and 705 cm^{-1} were also present.

We consider the wavelength dependence of the reaction. As shown in Fig. 2(a), upon $\lambda > 253.7$ nm irradiation only photoinduced isomerization from *anti*- to *syn*-CBA was observed. Subsequent $\lambda > 185.0$ nm irradiation caused the growth of the bands due to benzoyl chloride (Fig. 2(b)).

To clarify the route for benzoyl chloride formation (i.e., a radical or concerted process) a reactive O_2 matrix was used. Photoinduced isomerization from *anti*- to *syn*-CBA was observed, whereas photoinduced rearrangement was not as shown in Supplementary Fig. 1. As a result of the photolysis of O_2 upon 185.0 nm excitation, ozone was produced at 1037 cm^{-1} [16]. A strong band at 2342 cm^{-1} was assigned to CO_2 ν_3 [17]. Unfortunately, we could not determine the reason for the absence of the peaks due to benzoyl chloride. There remains the possibility that because of the filter effect of O_2, CBA did not absorb the 185 nm light that caused the rearrangement.

To study the reaction mechanism (section 3.2.), the photolysis of a benzoyl chloride/Ar matrix (1/1000) upon 185.0 nm excitation was conducted. Following the increase of a 2120 cm^{-1} band, the bands at 2139 (CO), 1088, 1024, 741 and 705 cm^{-1} increased. The wavenumbers of latter four bands are consistent with those of Ar-matrix-isolated chlorobenzene. The 2120 cm^{-1} band is tentatively assigned to C=C=O stretch of chlorocyclohexadienylidenemethanone. Growth behavior as shown in Supplementary Fig. 2 indicates chlorocyclohexadienylidenemethanone may serve as an intermediate species of chlorobenzene and CO photolysis products. It is confirmed that in the photolysis of the CBA/Ar matrix produced benzoyl chloride was further photolyzed.

3.2. Reaction mechanism

The decay behavior of *anti*-CBA and growth behavior of *syn*-CBA and benzoyl chloride are shown in Fig. 3. The *anti*- and *syn*-CBA show exponential decay and growth, respectively in which the absorbance of *anti*-CBA approaches a non-zero value, a profile typical for the reversible reaction. Benzoyl chloride exhibited no induction period to indicate its formation as the primary reaction product. However, the rate of formation of benzoyl chloride is slower compared with that of *syn*-CBA. The proposed reaction mechanism shown in Scheme I is based on the following assumptions: (1) a reversible reaction from *syn*- to *anti*-CBA exists, (2) the photolysis products of *anti*-CBA rapidly react to form benzoyl chloride and (3) benzoyl chloride undergoes photolysis. To confirm the mechanism shown in Scheme I, the rate constants k_1, k_2, k_3 and k_4 are estimated from the absorbance changes using the following rate equations:

$$\frac{dA_{anti}}{dt} = -(k_1 + k_3)A_{anti} + k_2 \frac{\varepsilon_{anti}}{\varepsilon_{syn}} A_{syn} \qquad (1)$$

$$\frac{dA_{syn}}{dt} = k_1 \frac{\varepsilon_{syn}}{\varepsilon_{anti}} A_{anti} - k_2 A_{syn} \qquad (2)$$

$$\frac{dA_{BC}}{dt} = k_3 \frac{\varepsilon_{BC}}{\varepsilon_{anti}} A_{anti} - k_4 A_{BC} \qquad (3)$$

where A and ε represent the absorbance and absorption coefficients, respectively. Subscripts anti, syn and BC refer to *anti*-CBA, *syn*-CBA and benzoyl chloride, respectively. The ratio of the absorption coefficients, $\varepsilon_{\text{anti}}$ (826 cm^{-1}):ε_{syn} (846 cm^{-1}):ε_{BC} (880 cm^{-1}), is assumed to be 1:1.1:7.3 on the basis of the DFT calculations. The rate constants k_1, k_2, k_3 and k_4 are estimated to be 0.0037 ± 0.00005, 0.00099 ± 0.00001, 0.00033 ± 0.00001 and 0.0034 ± 0.00005 min^{-1}, respectively. The fitted curves using the calculated values in Fig. 3 reproduce the observed absorbance changes satisfactorily.

The branching ratio of 12 (k_1/k_3) indicates that photoinduced rotational isomerization is the dominant reaction path rather than photoinduced rearrangement at the present excitation energy in the Ar matrix.

Table 2 lists the transition energies, oscillator strengths and transition characters of the singlet excited states of *anti*-CBA calculated at the TD-B3LYP/6-311++G(2d,2p) level. The calculated value of 3.52 eV for the $S_1 - S_0$ transition is slightly larger than the reported value of 3.21 eV by Haque and Thakur [18]. However, as shown in Supplementary Fig. 3, the absorption profile seems to be well reproduced by the TD-B3LYP calculation. Fig. 4 shows the molecular orbitals relevant to the transitions in Table 2. Table 3 lists the transition energies and characters of the triplet excited states of *anti*-CBA. Upon excitation at 185 nm (6.70 eV), *anti*-CBA is excited upto the S_{14} state. The S_1, S_2 and S_3 states are characterized as the (n, π^*), (π, π^*) and (π, π^*) states, respectively. Fig. 5 shows potential energy curves along the C–Cl bond length of the ground and low-lying excited states of *anti*-CBA. Under 4.89 eV (253.7 nm) vertical excitation energy, all states achievable are bound states. As the excitation energy increases the crossing points between the photoexcited state and the repulsive states become closer to the ground-state equilibrium geometry. Thus, *anti*-CBA in the excited singlet or triplet states after intersystem crossing will predissociate. Upon excitation at 6.70 eV (185.0 nm), direct excitation to the repulsive (π, $\sigma^*_{C–Cl}$) and (n, $\sigma^*_{C–Cl}$) states are possible. Photoinduced rearrangement will be caused by the reaction of thus dissociated cage pairs.

Conclusions

We have studied the 185 nm photolysis of *o*-chlorobenzaldehyde by infrared

spectroscopy in low-temperature Ar and O_2 matrices. In the Ar matrix, previously reported photoinduced rotational isomerization from *anti*- to *syn*-CBA was confirmed. In addition, absorption bands associated with photoinduced rearrangement to benzoyl chloride were observed accompanying the weak bands due to the CO photolysis product. Benzoyl chloride was further photodecomposed by the prolonged irradiation. In the reactive O_2 matrix, although isomerization was observed, there was no evidence for benzoyl chloride formation. A kinetic analysis revealed that the rearrangement was a minor process under the present excitation energy. The TD-B3LYP calculations showed that as the excitation energy increases the predissociation channel will open and the repulsive $^1(\pi, \sigma^*_{C–Cl})$ and $^1(n, \sigma^*_{C–Cl})$ states are directly achievable by the 185 nm excitation. Photoinduced rearrangement will be caused by the reaction of thus dissociated cage pairs.

References

[1] T. Ichimura, Y. Mori, H. Shinohara, N. Nishi, Chem. Phys. 189 (1994) 117.
[2] T. Ichimura, Y. Mori, H. Shinohara, N. Nishi, J. Chem. Phys. 107 (1997) 835.
[3] Y.-C. Tian, Y.-J. Liu, W.-H. Fang, J. Chem. Phys. 127 (2007) 044309.
[4] M.-F. Lin, C.-L. Huang, V.V. Kislov, A.M. Mebel, Y.T. Lee, C.-K. Ni, J. Chem. Phys. 119 (2003) 7701.
[5] R.N. Perutz, Chem. Rev. 85 (1985) 77.
[6] V.A. Apkarian, N. Schwentner, Chem. Rev. 99 (1999) 1481.
[7] R.N. Perutz, Chem. Rev. 85 (1985) 97.
[8] M.E. Jacox, F.L. Rook, J. Phys. Chem. 86 (1982) 2899.
[9] N. Akai, S. Kudoh, M. Takayanagi, M. Nakata, J. Photochem. Photobiol. A: Chem. 146 (2001) 49.
[10] N. Akai, S. Kudoh, M. Takayanagi, M. Nakata, J. Photochem. Photobiol. A: Chem. 150 (2002) 93.
[11] A.D. Becke, J. Chem. Phys. 98 (1993) 5648.
[12] C.T. Lee, W.E. Yang, R.G. Parr, Phys. Rev. B, 37 (1988) 785.

[13] M.J. Frisch, G.W. Trucks, H.B. Schlegel, G.E. Scuseria, M.A. Robb, J.R. Cheeseman, G. Scalmani, V. Barone, B. Mennucci, G.A. Petersson, H. Nakatsuji, M. Caricato, X. Li, H.P. Hratchian, A.F. Izmaylov, J. Bloino, G. Zheng, J.L. Sonnenberg, M. Hada, M. Ehara, K. Toyota, R. Fukuda, J. Hasegawa, M. Ishida, T. Nakajima, Y. Honda, O. Kitao, H. Nakai, T. Vreven, J. Montgomery, J. A., J.E. Peralta, F. Ogliaro, M. Bearpark, J.J. Heyd, E. Brothers, K.N. Kudin, V.N. Staroverov, R. Kobayashi, J. Normand, K. Raghavachari, A. Rendell, J.C. Burant, S.S. Iyengar, J. Tomasi, M. Cossi, N. Rega, N.J. Millam, M. Klene, J.E. Knox, J.B. Cross, V. Bakken, C. Adamo, J. Jaramillo, R. Gomperts, R.E. Stratmann, O. Yazyev, A.J. Austin, R. Cammi, C. Pomelli, J.W. Ochterski, R.L. Martin, K. Morokuma, V.G. Zakrzewski, G.A. Voth, P. Salvador, J.J. Dannenberg, S. Dapprich, A.D. Daniels, Ö. Farkas, J.B. Foresman, J.V. Ortiz, J. Cioslowski, D.J. Fox, Gaussian 09, Revision B.01, Gaussian, Inc.: Wallingford, CT,, (2010).
[14] D.A. Condit, S.M. Craven, J.E. Katon, Appl. Spectrosc. 28 (1974) 420.
[15] L. Andrews, J. Chem. Phys. 48 (1968) 972.
[16] S. Hashimoto, H. Akimoto, J. Phys. Chem. 91 (1987) 1347.
[17] T. Tamezane, N. Tanaka, H. Nishikiori, T. Fujii, Chem. Phys. Lett. 423 (2006) 434.
[18] M.K. Haque, S.N. Thakur, Indian J. Phys. 55B (1981) 477.

Figure captions

Fig. 1: (a) Infrared difference spectrum upon $\lambda > 185.0$ nm irradiation of the matrix CBA/Ar = 1/1000 for 120 min. Bands labeled by “s” and “a” are assigned to the absorption of *syn*-CBA and *anti*-CBA, respectively. “*” denotes artificial peaks. (b) Infrared spectrum of the matrix benzoyl chloride/Ar = 1/1000.

Fig. 2: Infrared difference spectra upon (a) $\lambda > 253.7$ nm irradiation for 60 min and (b) subsequent $\lambda > 185.0$ nm irradiation for 60 min of the matrix CBA/Ar = 1/1000. “*” denotes CO_2 in atmosphere.

Fig. 3: Absorbance changes of the *anti*-CBA (Δ), *syn*-CBA (○) and benzoyl chloride (□) upon $\lambda > 185.0$ nm irradiation of the matrix CBA/Ar = 1/1000.

Fig. 4: Relevant MOs of *anti*-CBA calculated at the TD-B3LYP/6-311++G(2d,2p) level.

Fig. 5: Potential energy curves along the C–Cl bond length of the ground and low-lying excited states of *anti*-CBA. The dashed and solid lines are used for triplet and singlet states, respectively.

Supplementary Fig. 1: Infrared difference spectrum upon $\lambda > 185.0$ nm irradiation of the matrix CBA/O_2 = 1/1000 for 300 min. "*" denotes artificial peaks.

Supplementary Fig. 2: Infrared difference spectra upon $\lambda > 185.0$ nm irradiation of the matrix benzoyl chloride/Ar = 1/1000 for (a) 15, (b) 60 and (c) 120 min.

Supplementary Fig. 3: Comparison of the experimental (solid line) and computed (stick) absorption spectra of CBA. The height of a stick represents the oscillator strength.

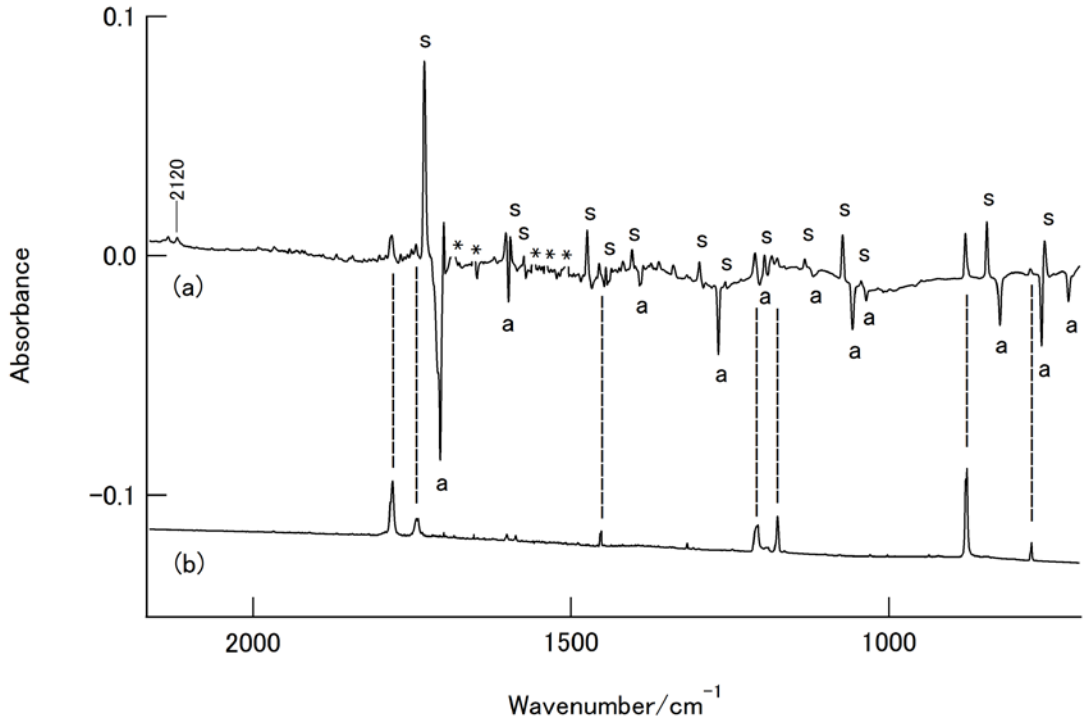

Fig. 1

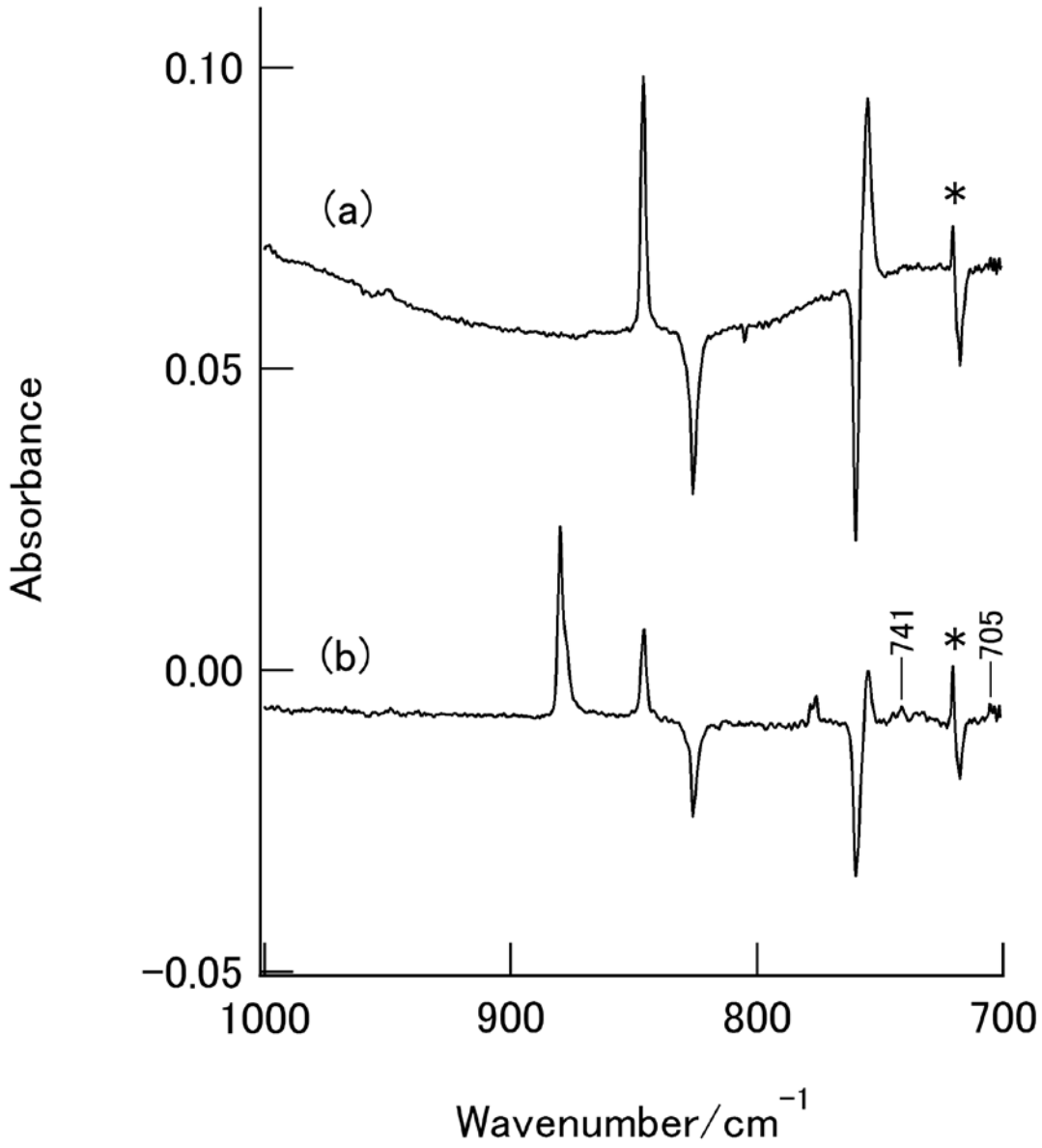
0.10
0.05
0.00
−0.05
Absorbance
(a)
(b)
*
*
741
705
1000
900
800
700
Wavenumber/cm^{-1}

Fig. 2

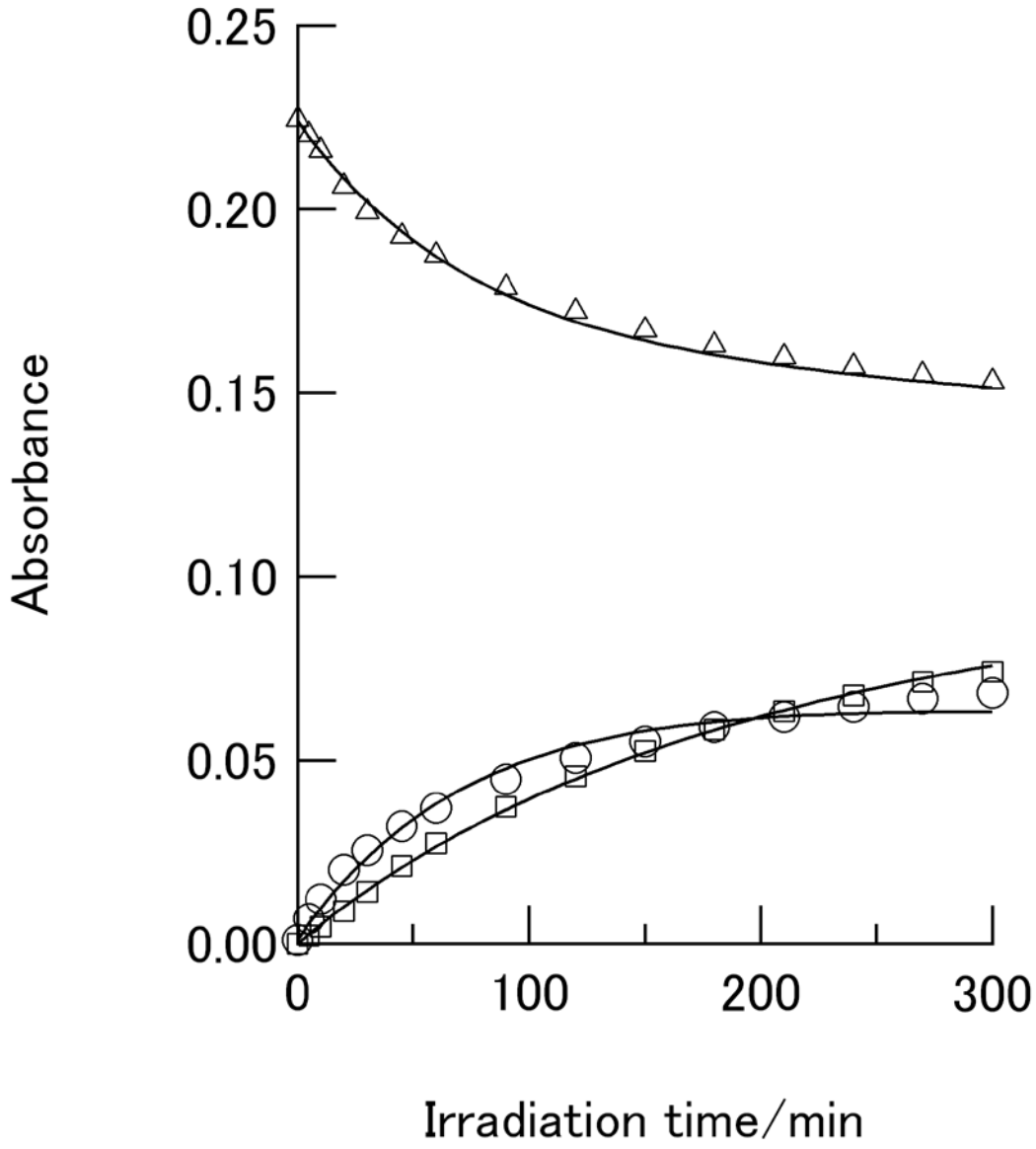
0.25
0.20
0.15
0.10
0.05
0.00
Absorbance
0
100
200
300
Irradiation time/min

Fig. 3

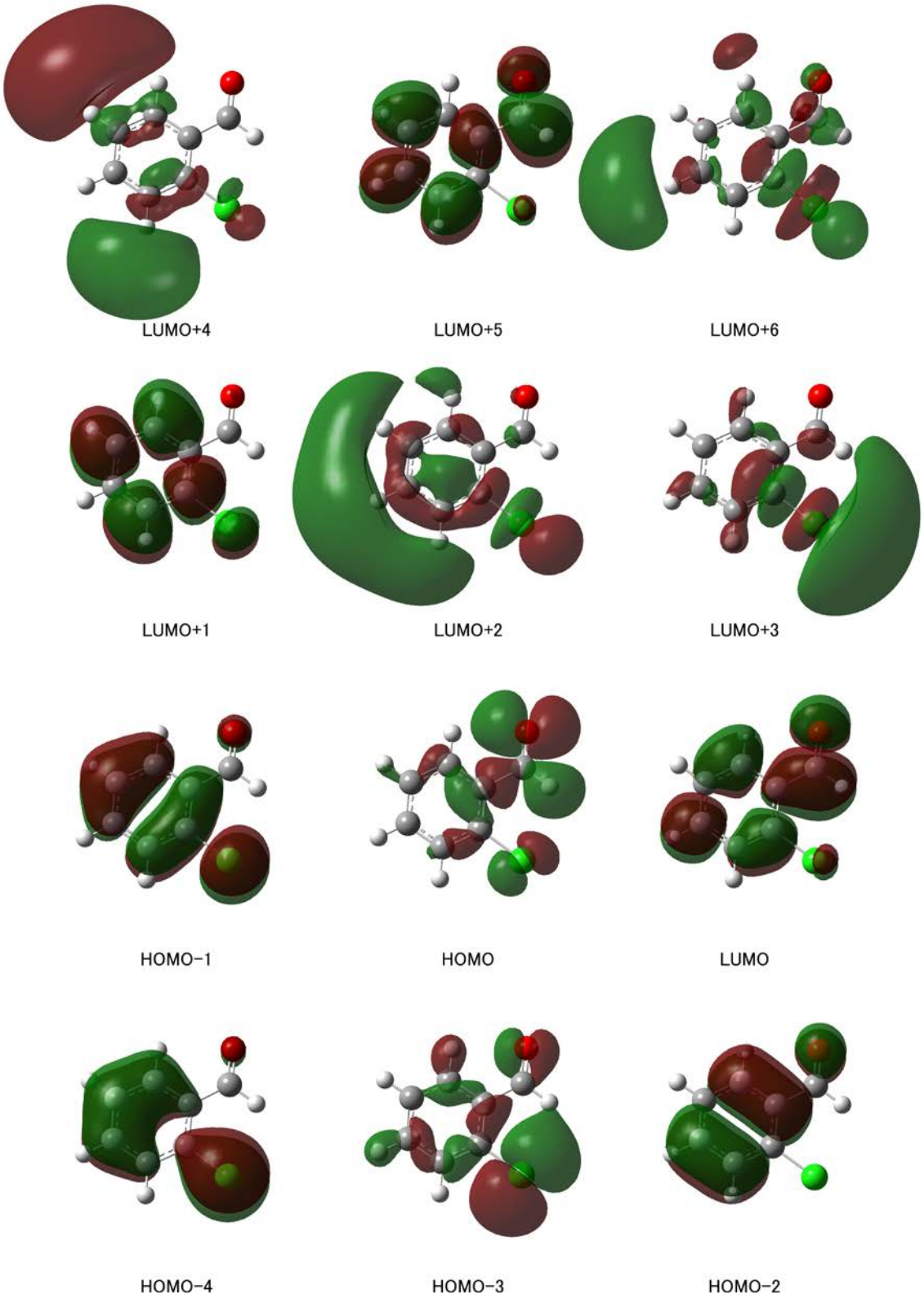
LUMO+4
LUMO+5
LUMO+6
LUMO+1
LUMO+2
LUMO+3
HOMO−1
HOMO
LUMO
HOMO−4
HOMO−3
HOMO−2

Fig. 4

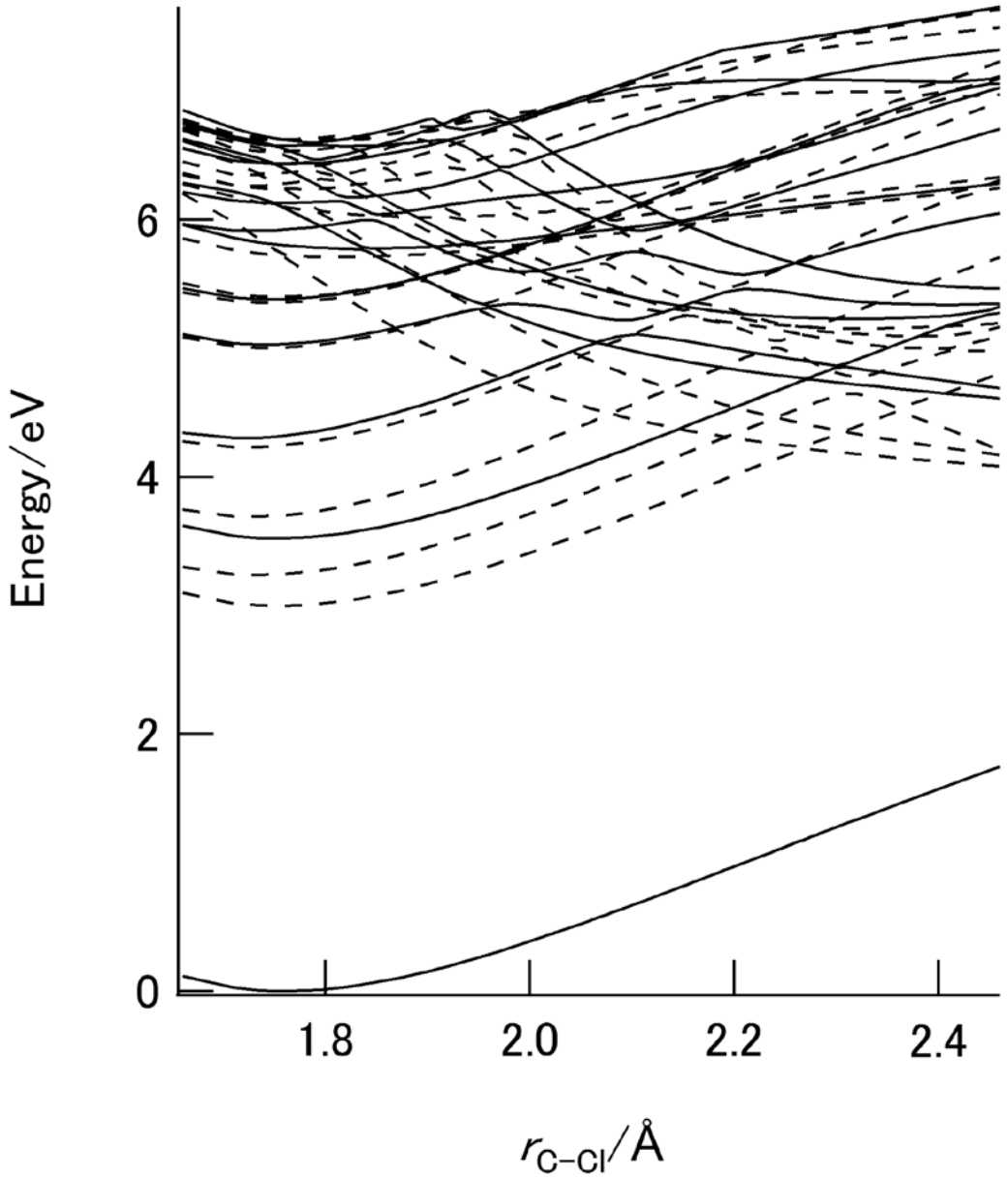

Fig. 5

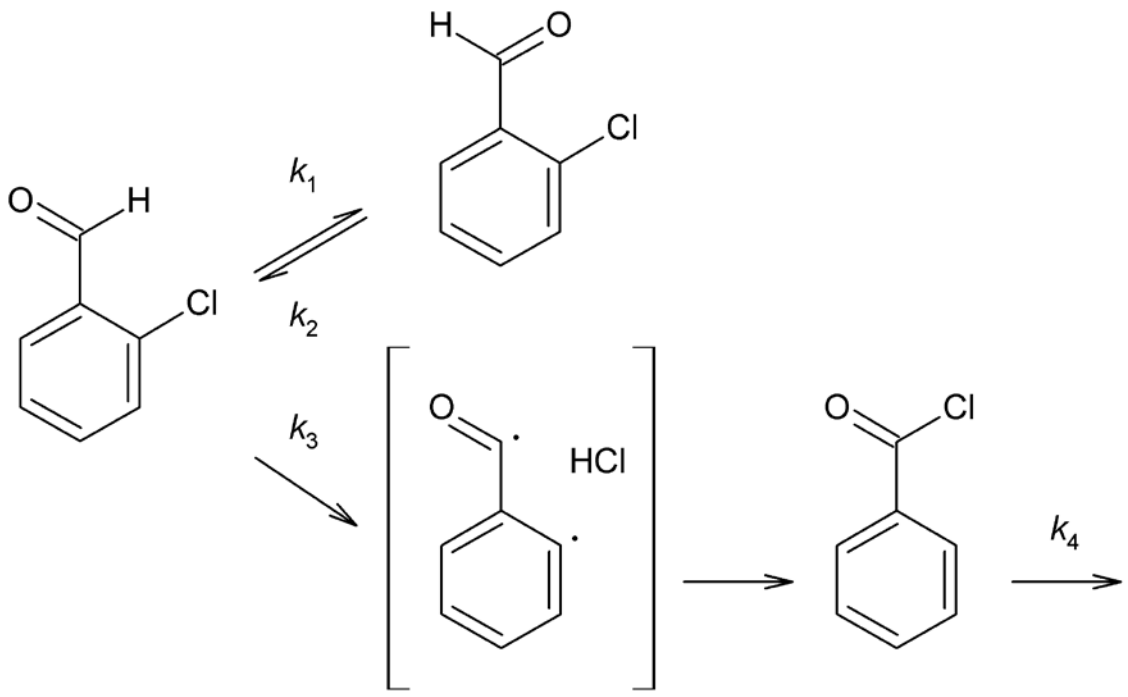

Scheme I

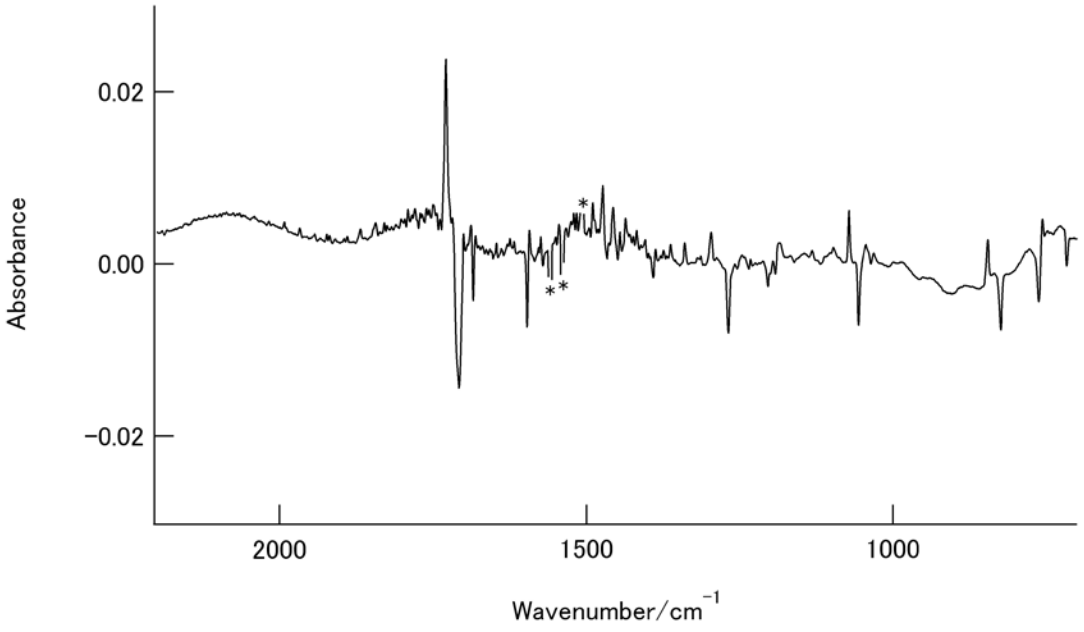

Fig. S1

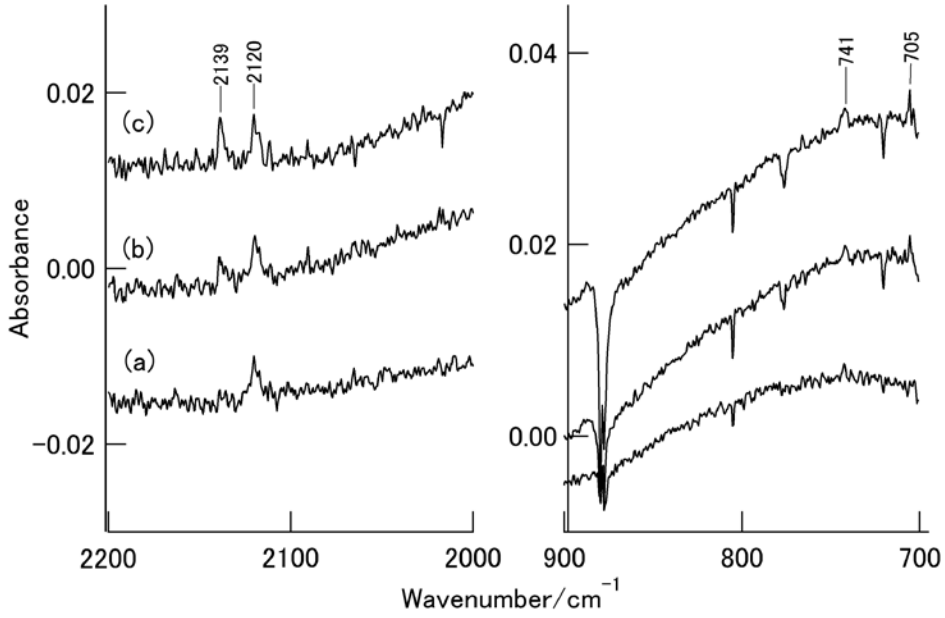
2139
2120
741
705
0.02
0.00
−0.02
0.04
0.02
0.00
(c)
(b)
(a)
Absorbance
2200
2100
2000
900
800
700
Wavenumber/cm^{-1}

Fig. S2

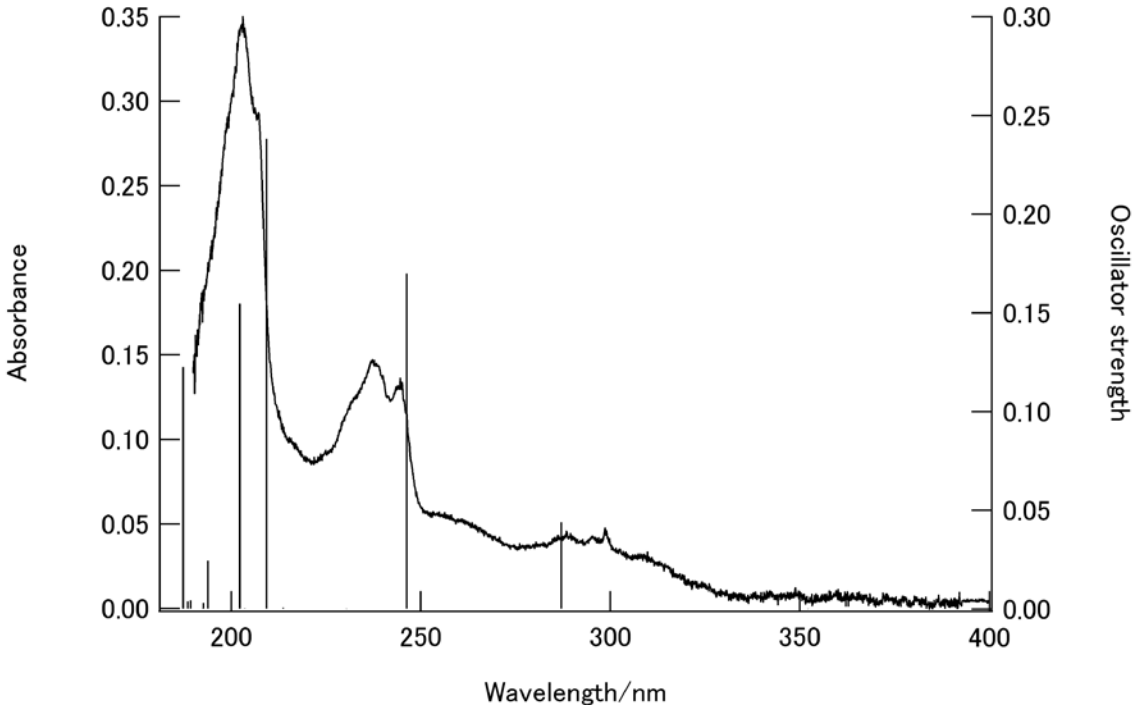
0.35
0.30
0.25
0.20
0.15
0.10
0.05
0.00
0.30
0.25
0.20
0.15
0.10
0.05
0.00
Absorbance
Oscillator strength
200
250
300
350
400
Wavelength/nm

Fig. S3

Table 1

Infrared spectra of photoproducts upon low-pressure Hg lamp irradiation of the CBA/Ar and CBA/O_2 matrices.

wavenumber/cm^{-1}		species
Ar	O_2	
2852		*syn*-CBA
2827		*syn*-CBA
2741		*syn*-CBA
2735	2731	*syn*-CBA
2728	2725	*syn*-CBA
	2342	CO_2
2139		CO
2120		*
1785		benzoyl chloride
1781		benzoyl chloride
1744		benzoyl chloride
1730	1729	*syn*-CBA
1596	1592	*syn*-CBA
1474	1473	*syn*-CBA
1455		benzoyl chloride
1445	1445	*syn*-CBA
1404	1404	*syn*-CBA
1317		benzoyl chloride
1300	1300	*syn*-CBA
1298	1296	*syn*-CBA
1257	1233	*syn*-CBA
1211		benzoyl chloride
1195	1195	*syn*-CBA
1184	1188	*syn*-CBA
1176		benzoyl chloride
1133	1131	*syn*-CBA
1074	1072	*syn*-CBA
	1037	O_3
1044	1032	*syn*-CBA
880		benzoyl chloride
846	845	*syn*-CBA

778		benzoyl chloride
776		benzoyl chloride
755	757	*syn*-CBA
741		*
705		*

*Photolysis products of benzoyl chloride.

Table 2

Transition energy, oscillator strength and transition character of the singlet excited states of *anti*-CBA calculated at the TD B3LYP/6-311++G(2d,2p) level.

state	energy/eV	oscillator strength	transition character
S_1	3.52	0.0001	0.70 (H → L)
S_2	4.32	0.0438	0.66 (H−1 → L)
S_3	5.03	0.1698	0.65 (H−2 → L)
S_4	5.38	0.0000	0.71 (H → L+1)
S_5	5.80	0.0006	0.69 (H−3 → L)
S_6	5.92	0.2379	0.51 (H−1 → L+1) − 0.36 (H−2 → L+1)
S_7	6.09	0.0004	0.61 (H−1 → L+2)
S_8	6.13	0.1546	0.45 (H−2 → L+1) + 0.39 (H−1 → L+1)
S_9	6.40	0.0246	0.59 (H → L+2) − 0.35 (H → L+3)
S_{10}	6.43	0.0030	0.63 (H → L+5)
S_{11}	6.44	0.0042	0.57 (H−1 → L+3)
S_{12}	6.55	0.0043	0.67 (H−2 → L+2)
S_{13}	6.57	0.0039	0.60 (H → L+3) + 0.33 (H → L+2)
S_{14}	6.62	0.1225	0.58 (H−4 → L)

Table 3

Transition energy and transition character of the triplet excited states of *anti*-CBA calculated at the TD B3LYP/6-311++G(2d,2p) level.

state	energy/eV	transition character
T_1	3.00	0.68 (H → L)
T_2	3.25	0.54 (H−2 → L) − 0.36 (H−1 → L)
T_3	3.70	0.59 (H−1 → L) + 0.35 (H−2 → L)
T_4	4.25	0.60 (H−1 → L+1)
T_5	5.01	0.65 (H−2 → L+1)
T_6	5.36	0.70 (H → L+1)
T_7	5.40	0.46 (H−7 → L) + 0.32 (H−2 → L+5)
T_8	5.70	0.41 (H−1 → L+2) − 0.36 (H−1 → L+3) − 0.35 (H−3 → L)
T_9	5.73	0.57 (H−3 → L)
T_{10}	6.10	0.57 (H−4 → L)
T_{11}	6.23	0.64 (H → L+5)
T_{12}	6.24	0.54 (H → L+2) − 0.37 (H → L+3)
T_{13}	6.28	0.60 (H−1 → L+5)
T_{14}	6.36	0.50 (H−1 → L+3) + 0.48 (H−1 → L+2)
T_{15}	6.50	0.66 (H−2 → L+2)
T_{16}	6.53	0.55 (H → L+3) + 0.38 (H → L+2)
T_{17}	6.62	0.57 (H−2 → L+5)
T_{18}	6.62	0.67 (H−5 → L)